

An Experimental Investigation of the Effects of Power Density and Surface Roughness in Glass-to-Metal Seals Material Processing

S. C. CHEN and K. VAFAI¹
Department of Mechanical Engineering
The Ohio State University
Columbus, OH 43210

Abstract: An experimental investigation of the glass-to-metal material processing for a hollow glass ampule is presented in this work. This investigation concentrates on the effects of the acting duration of the heat source, and the surface roughness of the metallic rod residing at the center of the glass tube. Several phenomenological features of the process are displayed and discussed. The present work does not follow the conventional research approach in the area of glass-to-metal seals rather it uses a non-conventional point of view to look at the phenomenological information on further understanding of the free surface movement and the occurrence of bubbles in glass-to-metal sealing processes. Detailed images of the actual sealing process provide valuable information on identifying and isolating the key regimes in the process and mapping out process defects, leading to a better understanding of the physical mechanisms involved in the sealing process. In addition, the flow field and free surface movement of the glass with respect to various power supplies and surface roughness of the metallic rod are also investigated in this work.

INTRODUCTION

THE manufacture of glass-to-metal seals is characterized by a high degree of empiricism. Furthermore, seal rejection and post manufacturing failures related to the process of forming the seal are quite common. Therefore, a practical need exists to reduce the empiricism in manufacturing the seal by a better understanding of the physics involved in the sealing process so that seal rejection and post manufacture problems can be minimized. This investigation is aimed at a basic understanding of some aspects of defects in the formation of seals through a systematic and carefully executed set of experiments. The present work does not follow the conventional research approach in the area of glass-to-metal seals rather it uses a non-conventional point of view to look at the phenomenological information on further understanding of the flow field and free surface movement of the glass with respect to various power supplies and surface roughness of the metallic rod and the occurrence of bubbles in glass-to-metal sealing processes.

Adhesion of glass to metal surfaces is a phenomenon of much importance in seal technology. Haim et al. [1] conclude that adhesion, which involves solidified glass, must begin with the wetting of the metal surfaces by the glass melt. They present an experimental method for comparing the tendency of glass melts to wet metal surfaces. Hrma [2] suggests a phenomenological theory for the formation of the interfacial bond between a glass and a solid, the analysis being based on the kinetics of adhesion. Wang et al. [3] conclude that, in addition to the surface energy between the solid and liquid phases, the cumulative effect of viscosity, interface condition and reaction on the surface is important for the wetting of glass on metal and that wetting and adherence can be improved by certain specific additives to the glass. Bhat et al. [4], Hoge et al. [5] and Brennan et al. [6] discuss several glass-metal systems and the effect of composition on the glass-metal interface reaction, wetting and adherence.

¹Author to whom correspondence should be addressed.
Paper received September 3, 1992.

NOMENCLATURE

D_i inner diameter of the glass tube (cm)	H height of the glass tube (cm)
D_o outer diameter of the glass tube (cm)	

As was pointed out in the work done by Chen & Vafai [7], glass and ceramic materials have become extremely useful in a variety of applications over the past few decades, especially in the electronic industry. Glasses are best suited for forming mechanically reliable and vacuum-tight fusion seals with metals, ceramics and micas, due to their properties, durability and formability. Vafai and Chen [8], had illustrated that the whole sealing process can be divided into three regimes. For the first regime, a glass tube is heated. This heating process is done by a laser beam in the present study. After reaching the softening, it enters the second regime. Because of the pressure difference induced over the outer surface [9] and the surface tension variation due to the temperature difference of the inner and outer free surfaces [10], the inner and outer surfaces start moving inwards, up to the point that the inner surface touches the conductor. After the inner surface touches the conductor, it enters the third regime of the sealing process.

Several aspects of the glass-to-metal seal have been under investigation for a long time. Buckley [11] and Miska [12] have presented a general glass-to-metal seals application guide. Some preliminary aspects of glass-to-metal sealing were discussed by Vafai [13]. It is quite important to note that very little work has been done in the systematic phenomenological understanding of the sealing process. The work done by Vafai and Chen [8] constitutes a detailed investigation of the free surface transport phenomenon inside the glass ampule employing the Marker and Cell (MAC) method. Later, an experimental investigation of free surface transport and subsequent bifurcation and adhesion for a hollow glass ampule was done by Chen and Vafai [7]. This work provided valuable information in identifying and mapping out process defects as well as providing some fundamental information in the area of free surface transport. In the present study, we are aiming at obtaining a further understanding of the formation of seals through a carefully designed systematic experimental investigation with different types of input power densities and different types of metallic conductors. In this work, images of five different sealing processes are presented, and valuable information is provided to understand the effects of the power density and the surface roughness of the metallic rod on the formation of the seal. In addition, the flow field and free surface movement of the glass with respect to various power supplies and surface roughness of the metallic rod are also investigated in this work.

EXPERIMENTAL APPARATUS AND PROCEDURE

The apparatus used in our experimental investigation is the set-up which is similar to the one used in the work of Chen and Vafai [7]. The hollow glass ampules used in the present study were manufactured by the Schott Technical Glass Company [14]. Thermal radiative absorption is desirable for these types of sealing processes and, for this reason, all of the glasses have a special coating (doped with FeO) which enables them to absorb most of the thermal radiation in the infrared range. The type of glass tube used in the present experimental investigation is 8530 from the Schott Technical Glass Company [14], with the inner diameter $D_i = 0.2642$ cm, outer diameter, $D_o = 0.3353$ cm and $H = 1.8136$ cm. The wavelength of the YAG laser is $1.064 \mu\text{m}$, which is in the infrared range. The chosen glass tube absorbs 85% of the radiation striking its surface at this wavelength.

The experimental set-up consists of the laser system, transmitting system, testing section, image processing system and control system. The laser used in the present experiment has an output power adjustable from 0 to 128 watts and changing the output power can be done by adjusting the laser lamp current. The lamp current is controlled and adjusted by the central pro-

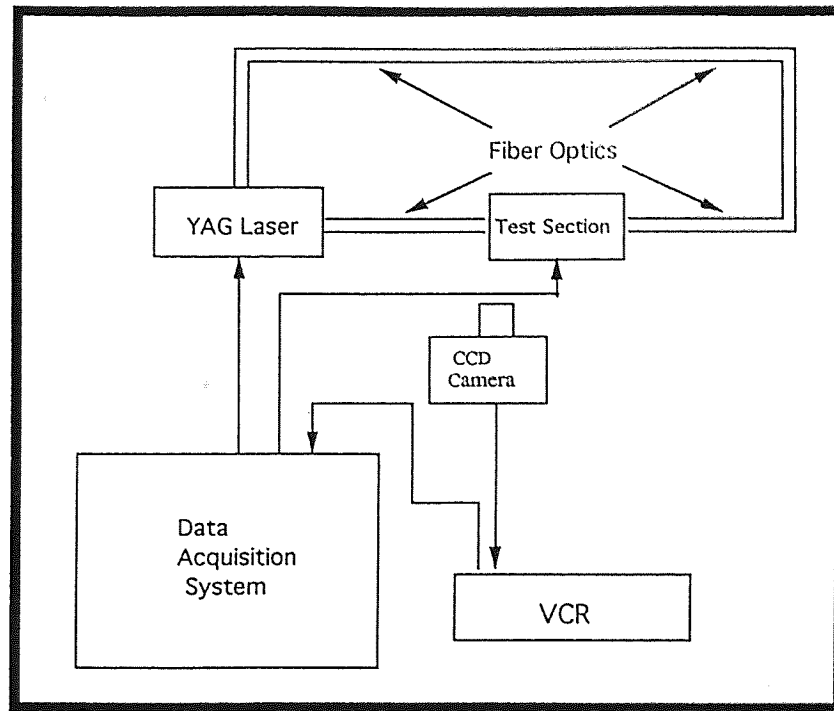


Figure 1a. Schematic diagram of the experimental set-up.

cessing unit with control signals sent out by the D/A converter within the data acquisition system. On receiving the command from the computer, the output power from the laser changes taking less than 100 ms to achieve steady output from the laser. In the present experiment, constant power supply is used in investigating the effect of the power density while ramping type of heat supply is employed in exploring the effect of the surface roughness. The laser beam is transmitted through a fiber optics system.

The test section is composed of two major parts: the holding mechanism and the rotating mechanism. A schematic diagram of the test set-up is shown in Figure 1a and schematic diagram of the sealing process is displayed in Figure 1b. The mechanism used to hold the glass ampule is a bracket with a clamp to adjust the inside diameter. The glass ampule is placed inside the bracket and is then tightened by the clamp. The position of the metal rod placed inside the glass

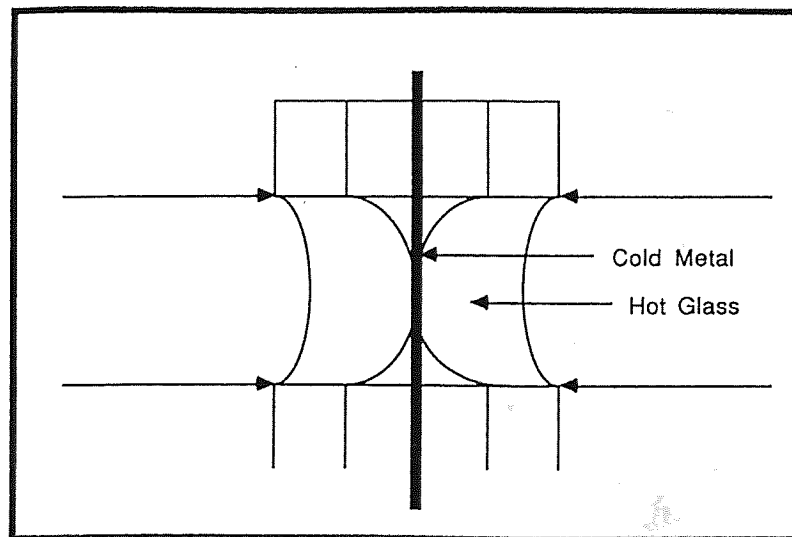


Figure 1b. Schematic diagram of the sealing process.

tube is an important parameter in the third regime of the sealing process. For this reason, three separate micropositioners are used to control the position of the metal rod more accurately. The output coupler of the fiber optics system is also an important mechanism, and is controlled by another micropositioner. This micropositioner controls the striking location of the laser beam on the glass tube and the subsequent amount of glass material fed into the core regime during the third regime of the sealing process. The other important purpose of this mechanism is to ascertain whether the laser beams are aligned with respect to each other. The output coupler micropositioner is adjustable in the z direction, allowing the range of striking locations to be from the center to the very top of the glass ampule. The effects of the striking location on the glass ampule, the location and angle of the metallic conductor, the ramping up or down of the power level and the magnitude of that power itself can be fully investigated by our present experimental set-up.

The CCD camera is used to track the movement of the glass ampule. We are interested in investigating the flow field and free surface movement of the glass with respect to various power supplies and surface roughness of the metallic rod. Based on some extensive preliminary tests, various initial settings for heating up the glass ampule to the melting point are explored. The CCD camera takes 30 frames per second and those images are monitored in real time during the sealing process. A frame-grabber is used for transferring the images from the CCD camera to the computer. Images from the CCD camera are first digitized and stored in the frame-grabber's memory, and then transferred to the computer using an RS-170 port.

The control system for the experimental set-up consists of the CPU unit, D/A board, frame-grabber and HP-3458A. The IEEE-488 interface and HP-3497A are not used in the present study because temperature field is not investigated. The control signals are sent from the master control unit through the D/A board to control the power density of the laser beam. Simultaneously, the HP-3458A is used to monitor the voltage output from the D/A board, where voltage is sent out of the control unit inside the laser control box to control the lamp current. The signal is sent to the CPU by the GPIB bus as a reference value.

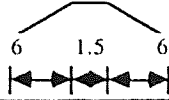
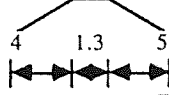
The experimental procedure was done in the following sequence. First, the heating characteristics were specified. For a specified incidence location of the laser beam, the CCD would then be adjusted. Next, the image processing program would be initialized. Finally, the master control program would be initialized, leading to the full execution of the experiment.

RESULTS AND DISCUSSION

Figures 2 to 6 are images taken by the CCD camera and then processed by our imaging system for five different cases. In the present work emphasis is placed on exploring the lower power density of heat source and the effects of surface roughness of the metallic rod. For the first part of the present study, a metallic rod without any surface roughness is used. In this work an extensive comparison between using metal rod with significant surface roughness and a rod without surface roughness is made to investigate these effects on the free surface movement during the sealing process. Figures 2 to 4 are based on cases which were chosen after many experiments such that they would reveal pertinent information with respect to the effects of the power level and the incidence location on free surface transport, and bifurcation of the glass material when it touches the metal rod and adhesion phenomena for the glass ampule and the glass-to-metal seal formation. Figures 5 and 6 reveal important information on the effect of the surface roughness on the occurrence of bubbles inside the seal. The heating input characteristics, the incidence locations, and the specific observations are displayed in Table 1.

For case 1, as shown in Figure 2, the laser beam strikes the outer surface of the glass ampule, causing the temperature increase within the glass ampule. Due to the variation of the surface tension difference caused by the temperature difference across the film as shown in Vafai and Chen [8], the temperature of the glass reaches the softening point, and the inner and outer free surfaces are no longer in an equilibrium state. As a result, the inner and outer surfaces will move until they reach an appropriate equilibrium state. In the absence of an external force to

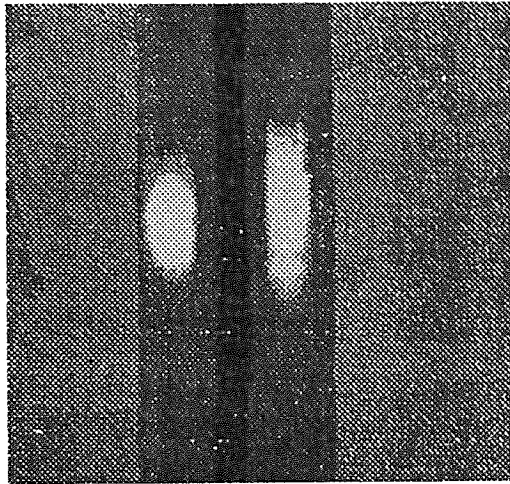
TABLE 1. Input Information for Cases 1 to 5.

Case	Related Figures	Input Power (watt)	Heating Characteristics	Incidence Location (mm) (from top end)	Observations
1	1I, 1II	7.5	Constant Power Supply	3.0	Loose Seal
2	2I, 2II 2III	12	Constant Power Supply	3.0	Single Bubble Formation
3	3I, 3II	15	Constant Power Supply	3.0	No Bubble Formation
4	4I, 4II 5III	28		6.0	Bubble Formation
5	5I, 5II 5III, 5IV	28		6.0	No Bubble Formation

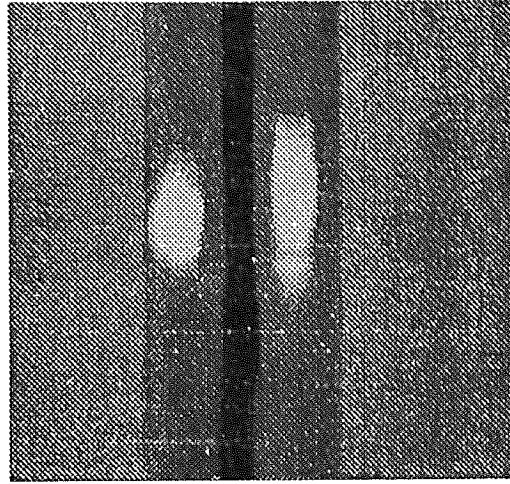
drive the motion, the film will arrive at a new steady state position such that a new balance between the surface tension force, the gravitational force and the applied pressure difference will be re-established. However, the inner surface will keep on moving if there is an external force, such as the feed-in mechanism through the upper boundary. For case 1, due to the low input power from the laser and low thermal radiation pressure induced by the low input power from the laser, a premature equilibrium state is achieved and consequently, the inner surface stops moving inwards. The premature equilibrium here is referring to the fact that due to the low input power the sealing process is not completed. This can be seen clearly in Figure 2(II).

There are two ways to re-establish a new equilibrium state for case 1: more laser power input to induce more pressure difference, and/or larger inflow from the upper part of the glass ampule. Referring to Figure 2, it is seen that there is not much inflow coming from the upper boundary since all the heat from the laser is taken up by natural convection and high thermal radiation from the free surfaces caused by the large temperature difference between the environment and the glass ampule, and only a very small portion of radiation energy can reach the upper boundary by way of heat conduction. Low heat flux on the outer surface translates into a low thermal radiation pressure resulting in a lower quantity of the glass material above the core region to reach the melting temperature. This causes a low inflow velocity from the upper boundary. For case 1, due to this low inflow velocity from the upper boundary, it will take more than 10 minutes for the inner free surface to touch the metal. But, since the experiment was terminated before 10 minutes had elapsed, the inner surface of the glass ampule will not touch the metal rod. Therefore, the sealing process can still be accomplished for longer times, however, for mass production, the cost of the product will increase significantly. It should be also noted that the inner free surface has not touched the metal rod so the surface condition of the rod had no effect on the flow field for case 1.

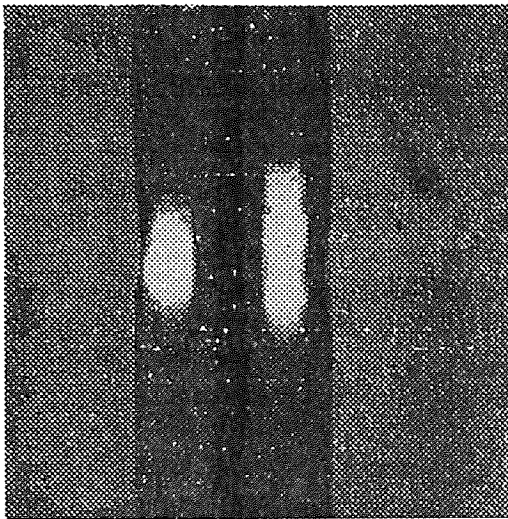
Based on the outcome of case 1, the input power from the laser was increased for case 2 using the same type of heating characteristics used in case 1. As seen in Figure 3, the inner free surface of the glass ampule touches the metal rod at a time equal to $t = 9.37$ seconds after the laser beam starts striking the outer surface of the glass ampule. Compared to the higher power density and lower incidence locations, it takes more time in this case for the inner surface to touch the metal rod due to a lower influx from the upper boundary and a lower pressure difference which in turn is due to a lower power density incident on the outer surface. For this case the inner surface of the glass piece moves in faster compared to the previously discussed case 1, however, there is a large bubble formed at the center of the seal.



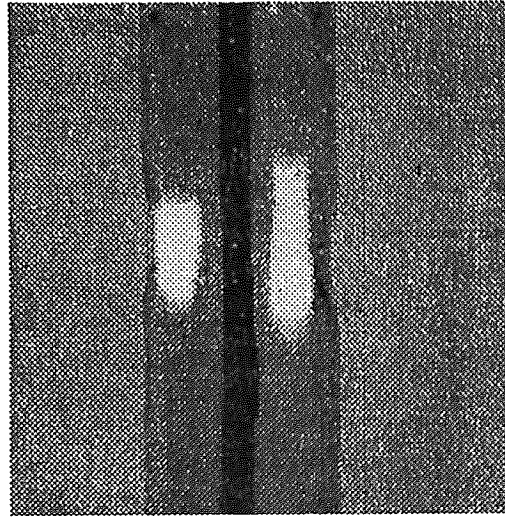
(a) $t = 6.72$ Sec.



(b) $t = 7.40$ Sec.



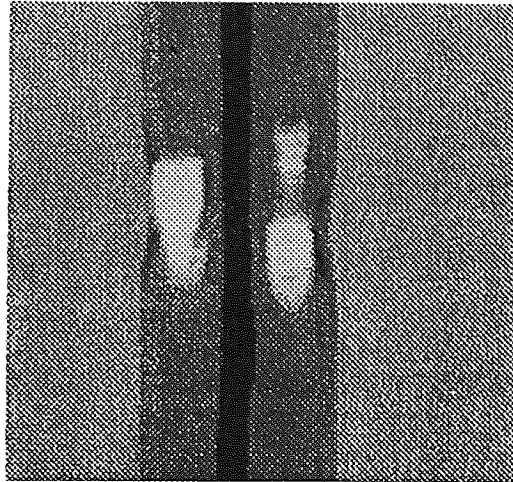
(c) $t = 10.84$ Sec.



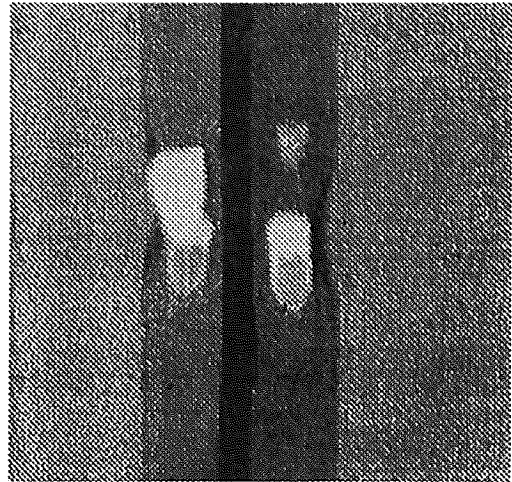
(d) $t = 14.44$ Sec.

(I)

Figure 2. Images displaying the formation of a loose seal for case 1.



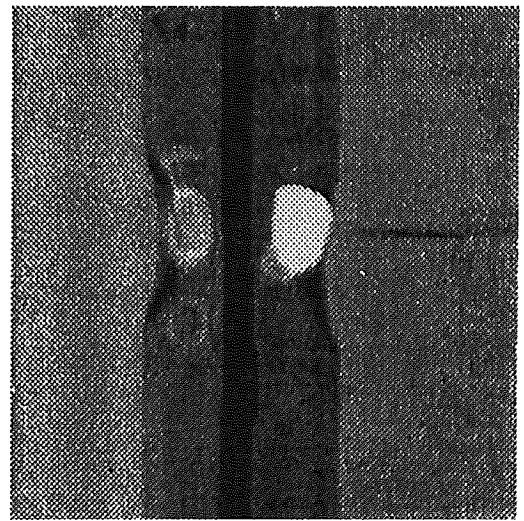
(e) $t = 16.61$ Sec.



(f) $t = 17.39$ Sec.



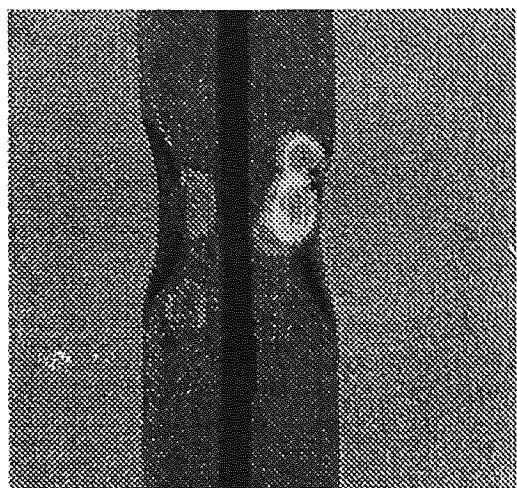
(g) $t = 23.34$ Sec.



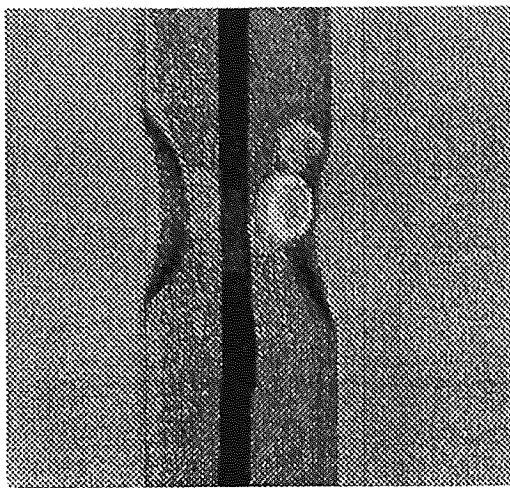
(h) $t = 32.24$ Sec.

(II)

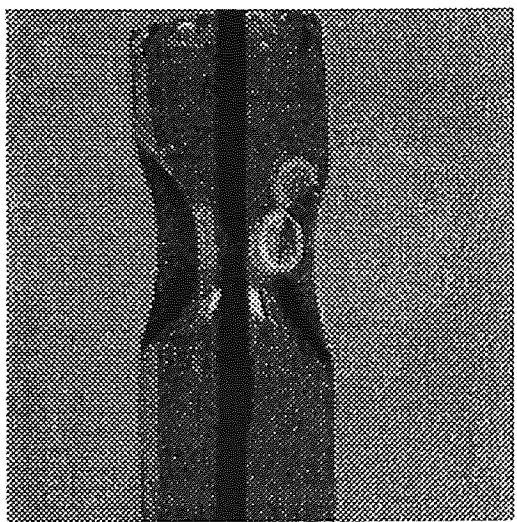
Figure 2 (continued). Images displaying the formation of a loose seal for case 1.



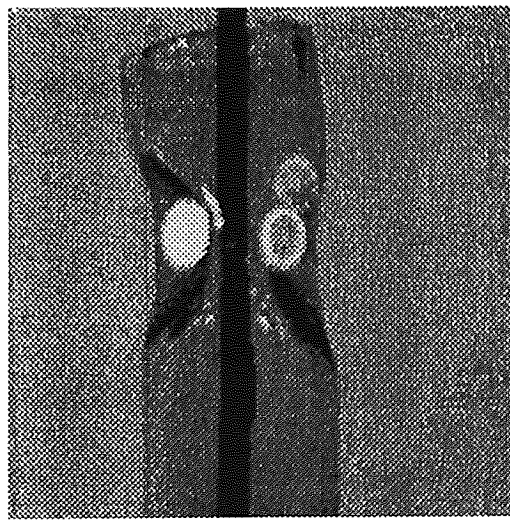
(j) $t = 49.88$ Sec.



(k) $t = 56.07$ Sec.



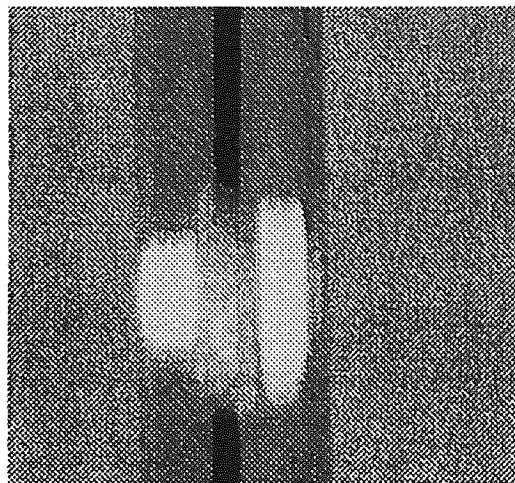
(l) $t = 114.91$ Sec.



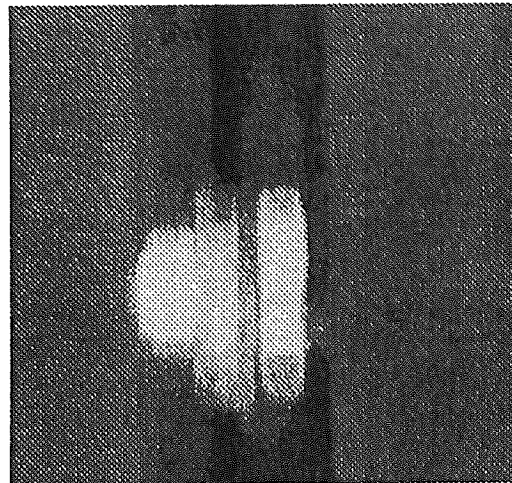
(m) $t = 156.37$ Sec.

(III)

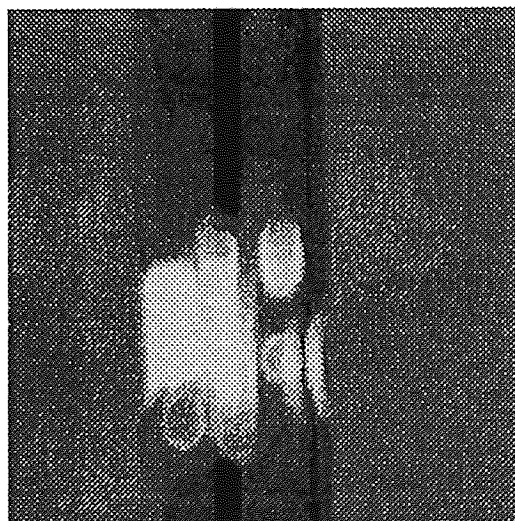
Figure 2 (continued). Images displaying the formation of a loose seal for case 1.



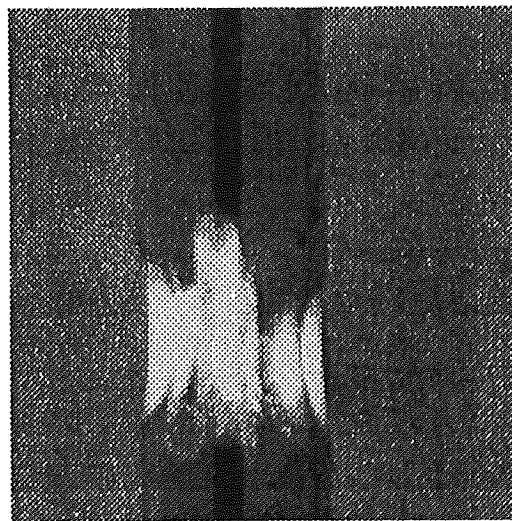
(a) $t = 1.63$ Sec.



(b) $t = 2.42$ Sec.



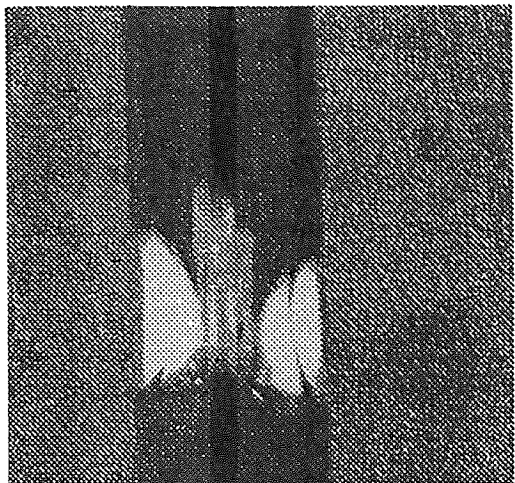
(c) $t = 4.58$ Sec.



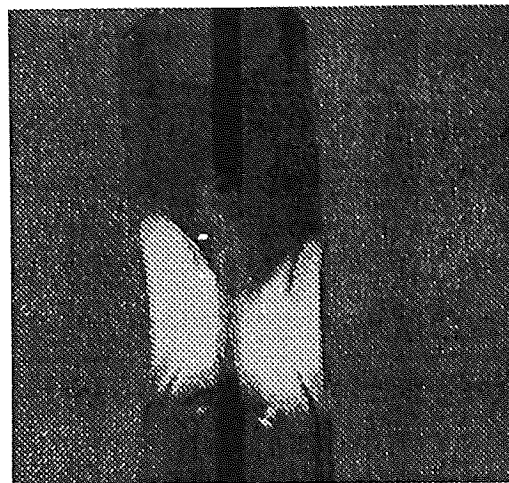
(d) $t = 6.02$ Sec.

(I)

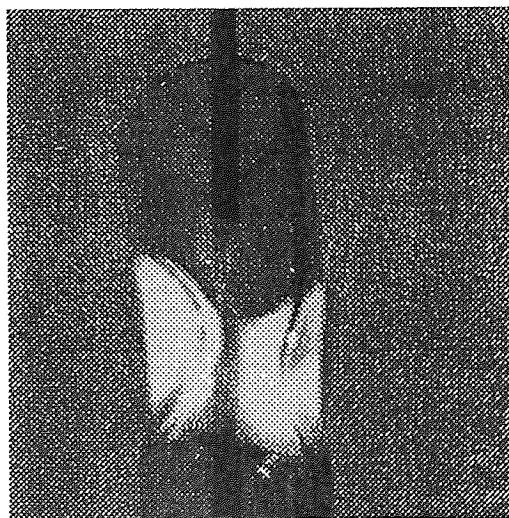
Figure 3. Images representing the single bubble formation in case 2.



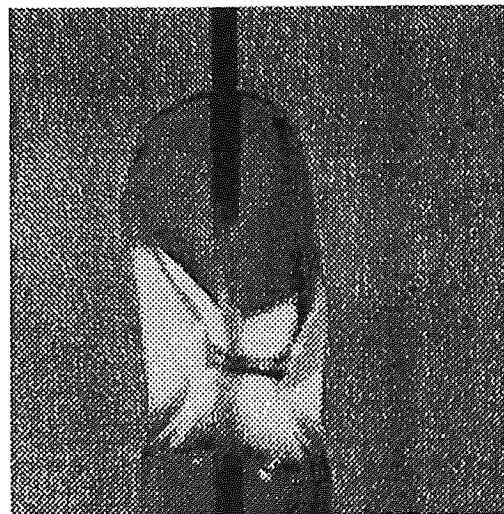
(e) $t = 6.50$ Sec.



(f) $t = 9.37$ Sec.



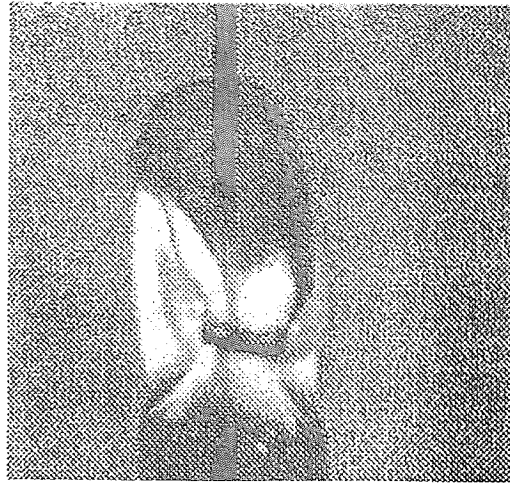
(g) $t = 11.01$ Sec.



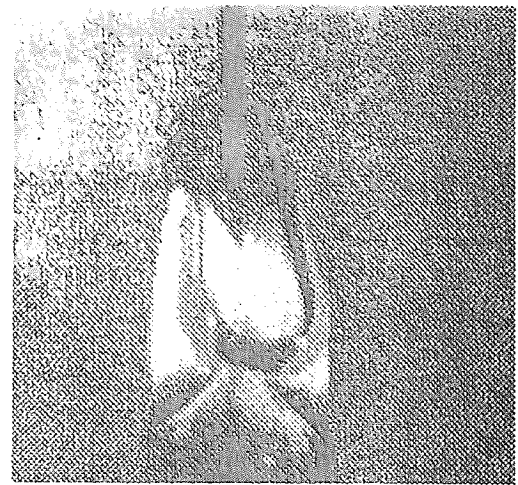
(h) $t = 12.35$ Sec.

(II)

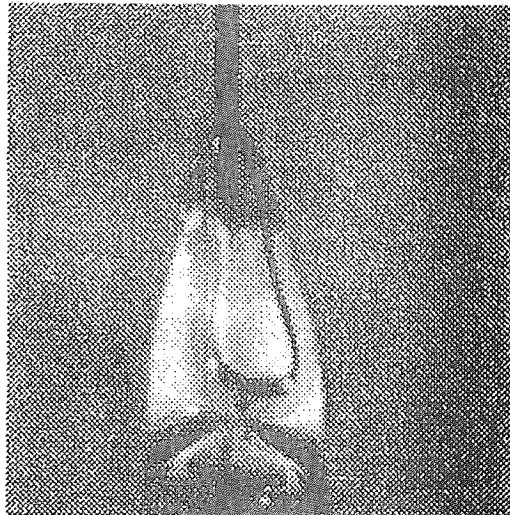
Figure 3 (continued). Images representing the single bubble formation in case 2.



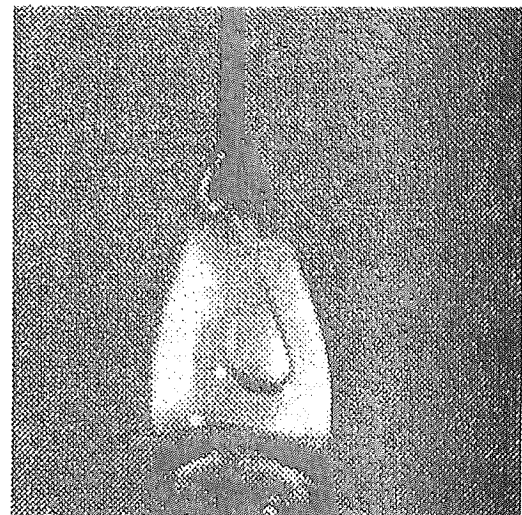
(l) $t = 14.77$ Sec



(m) $t = 19.27$ Sec

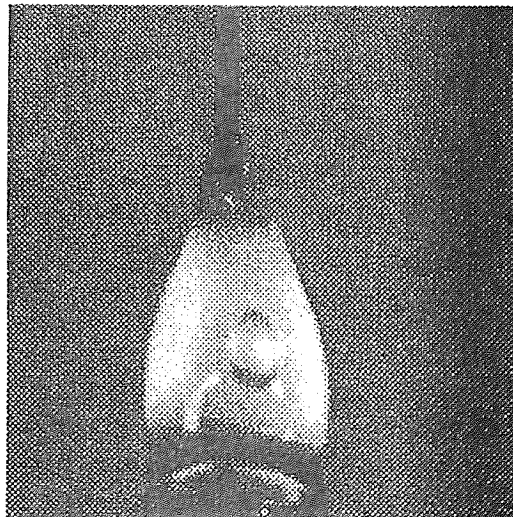


(n) $t = 21.26$ Sec

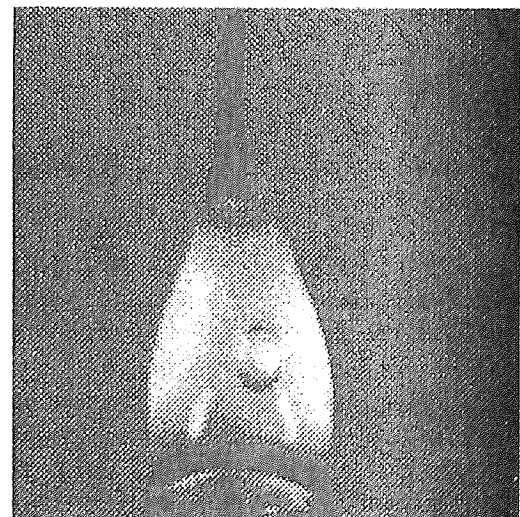


(o) $t = 23.07$ Sec

(III)



(p) $t = 25.43$ Sec



(q) $t = 26.32$ Sec

(IV)

Figure 3 (continued). Images representing the single bubble formation in case 2.

The mechanisms for formation of a bubble, can be explained from the heat supply point of view. Referring to Figure 3, a cavity shows up at $t = 11.01$ sec, and shrinks gradually because glass material from the upper part keeps feeding into the cavity and fills the space which was previously filled with air. Due to the incidence location of the laser beam initially, no more glass material (the amount is mainly determined by the incidence location of the laser beam) can be fed into the core regime at time equal to 13 seconds, when there is still a bubble inside the core regime. The required extra inflow of the glass material requires a greater energy supply, which means more time is needed if the same power density is used. Another reason for the bubble formation can be because of the natural convective currents which are due to the large temperature difference between the surface of the glass ampule and the ambient air. The natural convection effects are not significant for processes which require a shorter heating duration. This is because for shorter duration applications there is not enough time for the natural convection to play a role in the process.

However, for case 2, lower power density results in a longer duration for the sealing process and so the natural convection effects become significant. Furthermore, as the glass material feeds into the air cavity, it will experience a larger retardation force caused by higher degree of disturbance of the air within the cavity. Referring to Figure 3, symmetric motions of the free surfaces are obtained at the beginning and, as time goes on, asymmetric motion of the free surfaces commences. This phenomenon will increase the chance of bubble formation because incoming material is no longer fed into the spot where the cavity formerly resided.

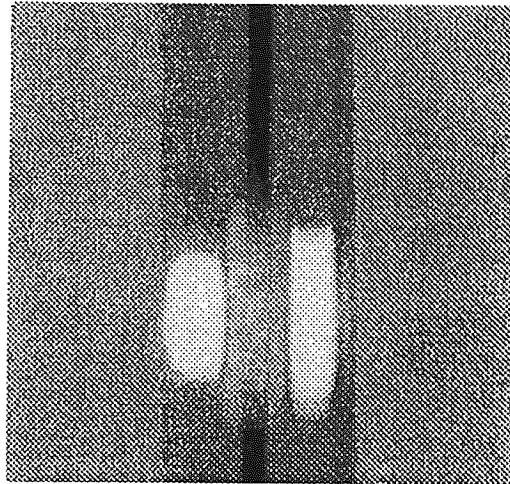
To shrink the required time for eliminating the bubble, a higher power supply from the laser beam is implemented. Referring to Figure 4, the bubble has been eliminated and the quality of the seal is now significantly better than the former two cases. The sealing characteristics for case 3 are listed in Table 1. As seen in Figure 4, glass material is gradually fed into the core region, and there is no cavity formed during the whole sealing process. Therefore, it is plausible to expect no bubble, if enough glass material from the upper part is fed into the cavity. Cases 2 and 3 have made it amply clear that the lack of heat supply at the final stage is the major reason for a loose seal and bubble formation.

The rods used in cases 1 to 3 are different from those used in the work of Chen and Vafai [7]. In their work, the rods had some artificial surface roughness while the rods used for the above cases were made without any surface roughness. For some applications, depending on the level of stress the seal has to sustain, surface roughness is introduced intentionally to enhance the strength of the glass-to-metal seals. For example, a proper size and distribution of the roughness over the surface, serves as a strengthening mechanism for the seal.

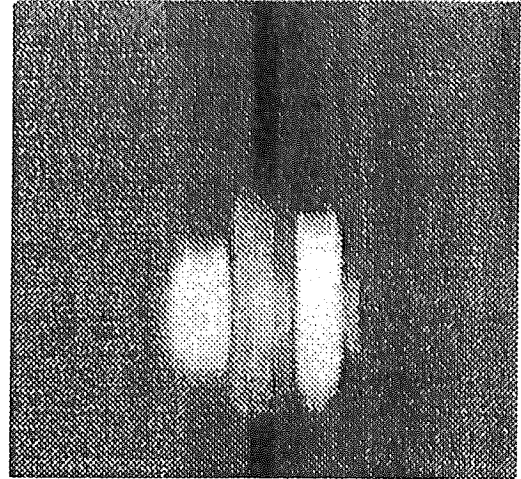
On the other hand, an improper size and/or distribution could adversely affect the flow field within the seal resulting in a product defect. Cases 4 and 5 are implemented to explore these surface roughness effects on the flow field during the sealing process. Referring to Figure 5(I), a bump on the surface of the metallic rod can be seen. This type of surface roughness could cause a product defect instead of increasing the quality of the seal. The heating input characteristics, the incidence locations, and the power level for cases 4 and 5 are listed in Table 1.

It should be noted that the incidence locations for cases 4 and 5 are lower than cases 1 to 3. The incidence location is 6 mm from the top for cases 1 to 3. The reason for lowering the incidence location is to create more material feeding into the center regime to clearly observe the effects of the big bump [referring to Figure 4(I)] on the flow field. A higher power is used to reduce the sealing process duration in order to avoid the possible instability introduced with longer process time as discussed in relation to case 2. Furthermore, higher powder density of the heat source minimizes the natural convection effects.

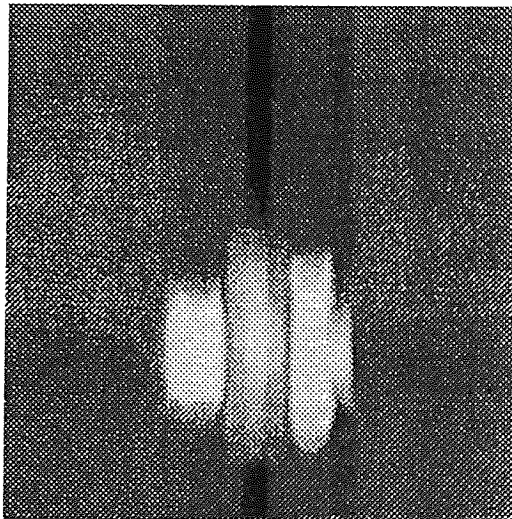
For case 4, a loose seal was obtained with a single bubble formation. As seen in Figure 5(II), at $t = 8.17$ seconds, a relatively large cavity is formed in the vicinity of the bump. As the process proceeds, glass material coming from the top is expected to feed into and fill the space. However, due to the existence of the bump, the flow of the feed-in glass material is retarded and diverted by the sheer size of the bump. The glass material moving in the direction perpendicular to the bump is stagnated on top of the bump. As the process proceeds, more glass material is stacked at the top of the bump resulting in a lower quantity of glass material above the core re-



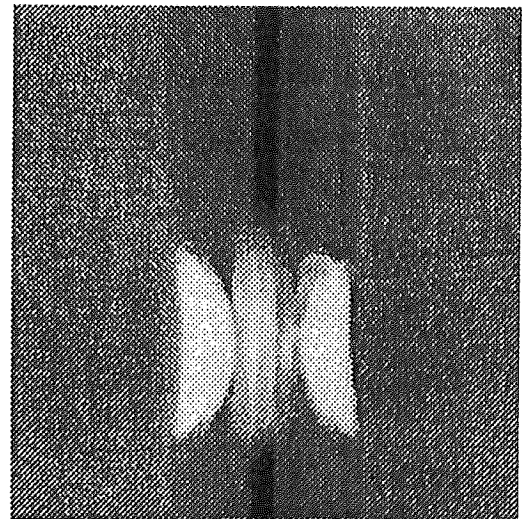
(a) $t = 0.81$ Sec.



(b) $t = 1.44$ Sec.



(c) $t = 2.08$ Sec.



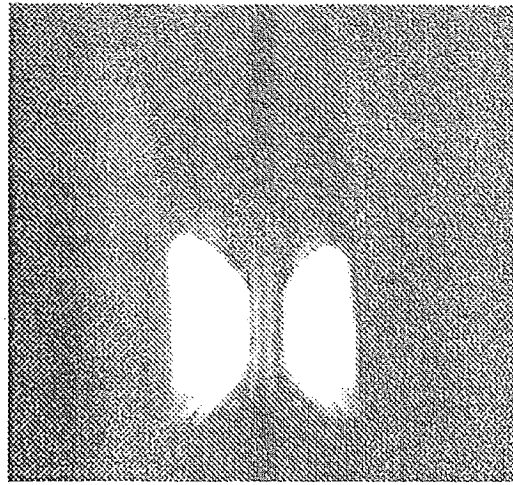
(d) $t = 3.60$ Sec.

(1)

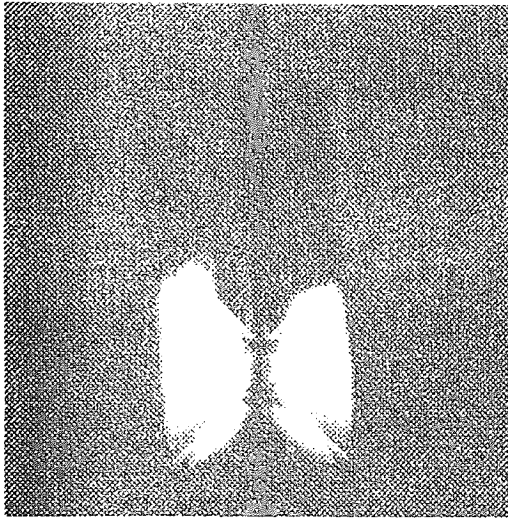
Figure 4. Effects of higher power density (case 3) in removing the bubble formation shown in case 2.



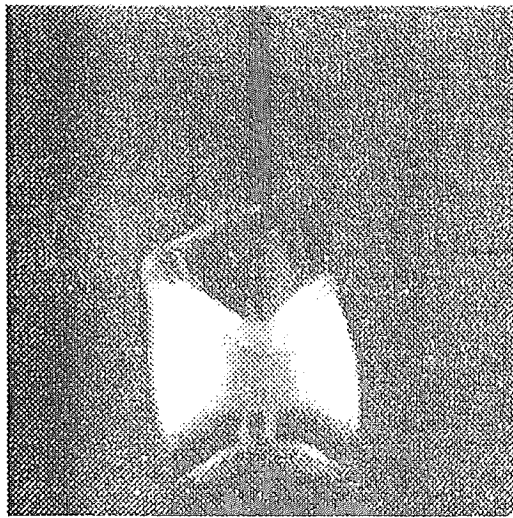
(a) $t = 4.55$ Sec



(b) $t = 5.67$ Sec

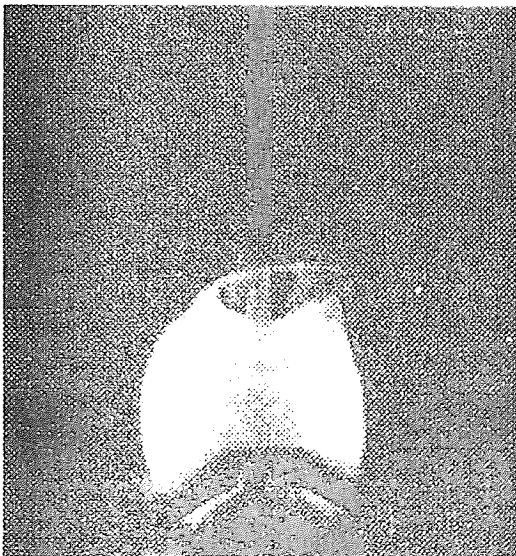


(c) $t = 7.45$ Sec

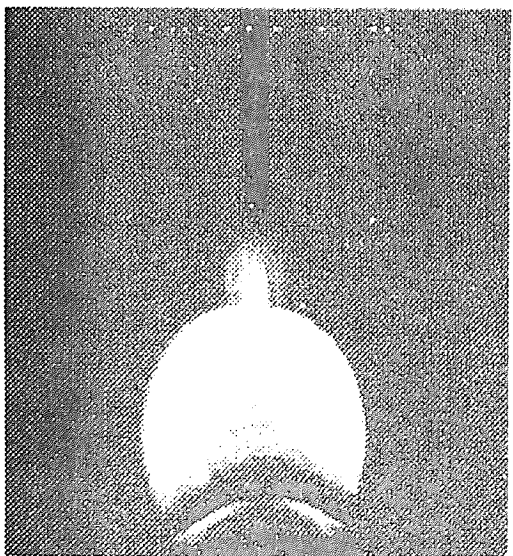


(d) $t = 9.07$ Sec

(II)



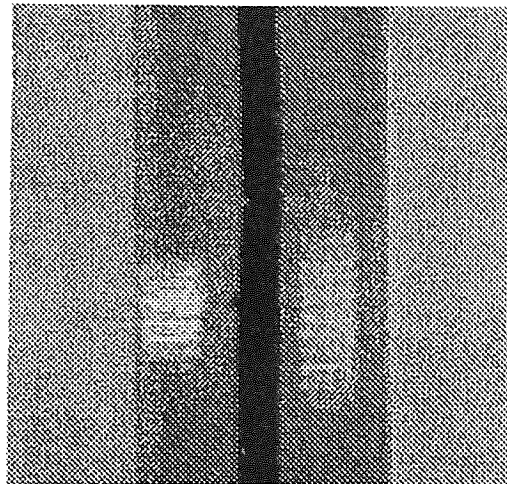
(e) $t = 10.82$ Sec



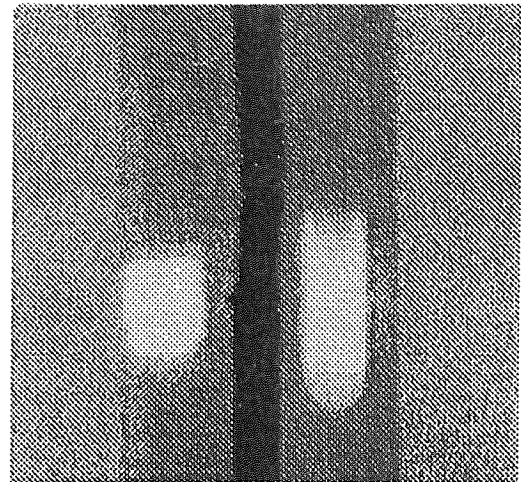
(f) $t = 12.77$ Sec

(III)

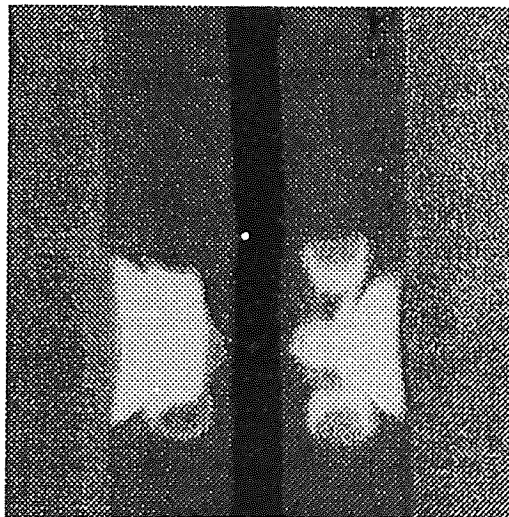
Figure 4 (continued). Time sequence of laser light sheet showing the growth of laser-induced flow in case 2.



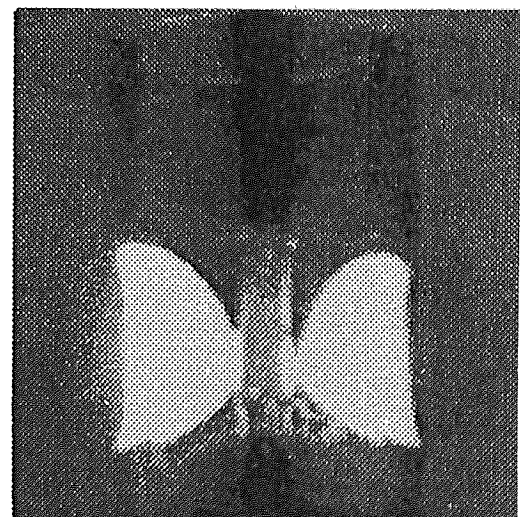
(a) $t = 0.36$ Sec.



(b) $t = 1.59$ Sec.



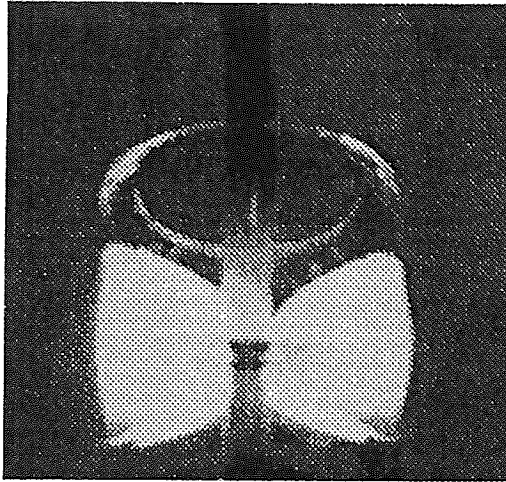
(c) $t = 5.31$ Sec.



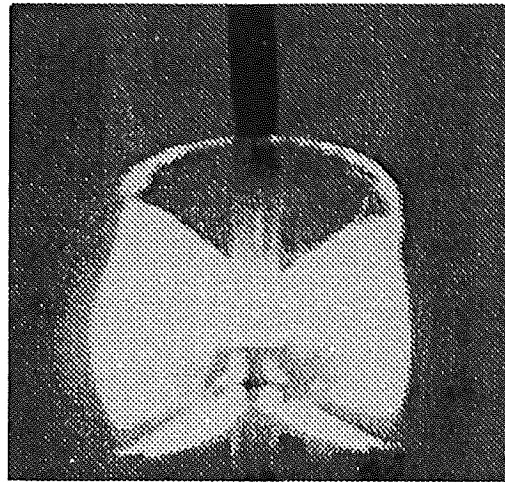
(d) $t = 7.00$ Sec.

(l)

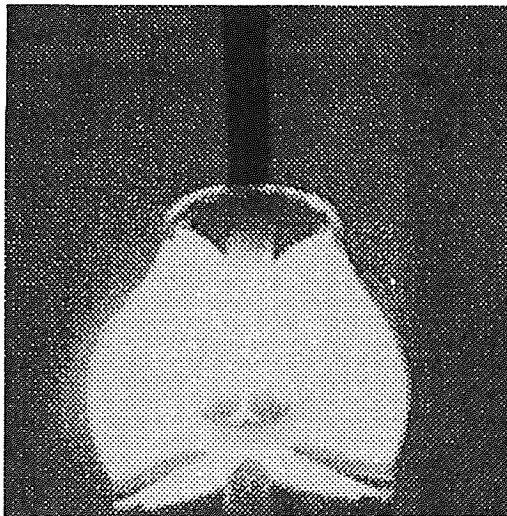
Figure 5. Effects of the surface roughness on the sealing process (case 4).



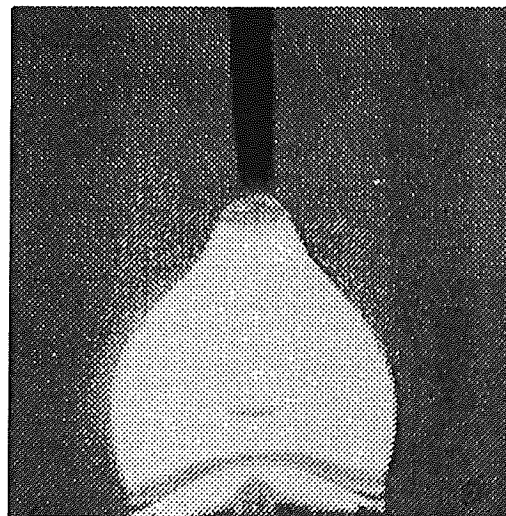
(e) $t = 8.17$ Sec.



(f) $t = 8.67$ Sec.



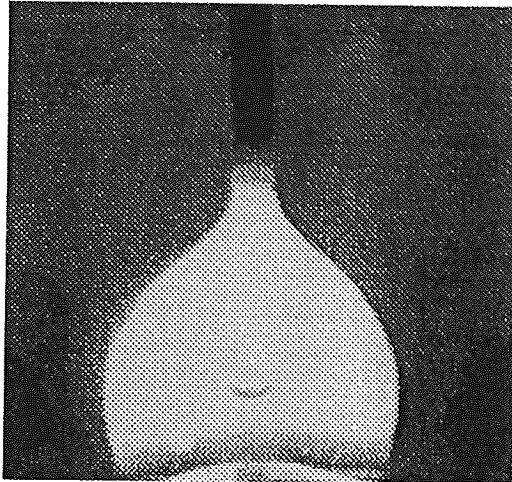
(g) $t = 9.09$ Sec.



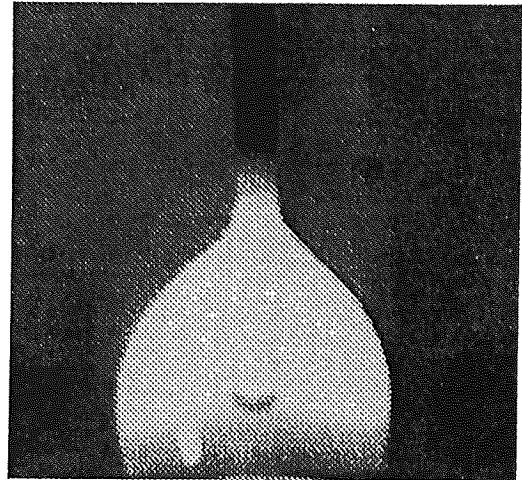
(h) $t = 9.62$ Sec.

(II)

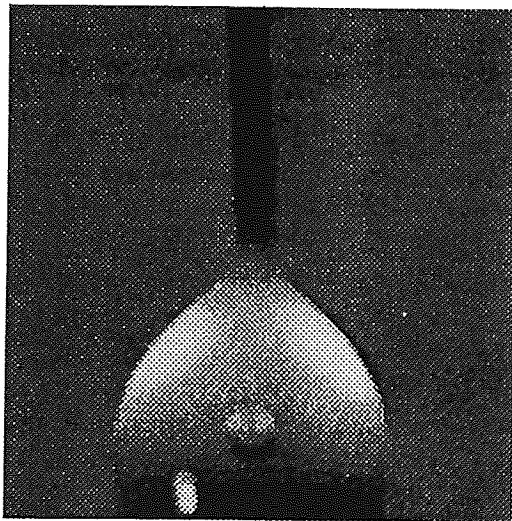
Figure 5 (continued). Effects of the surface roughness on the sealing process (case 4).



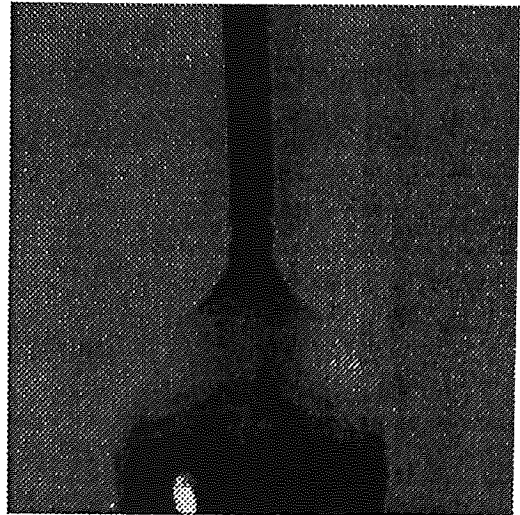
(a) $t = 11.22$ Sec.



(b) $t = 12.60$ Sec.



(c) $t = 14.04$ Sec.



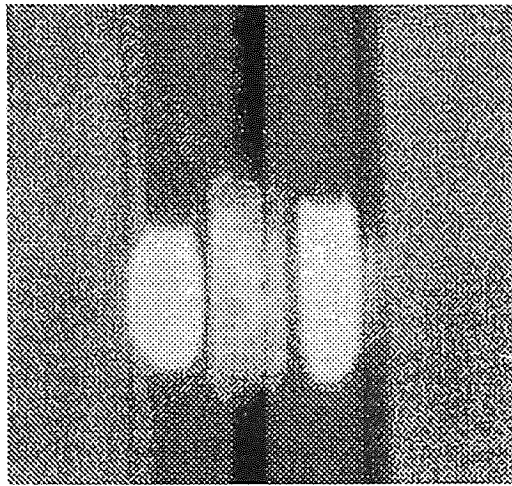
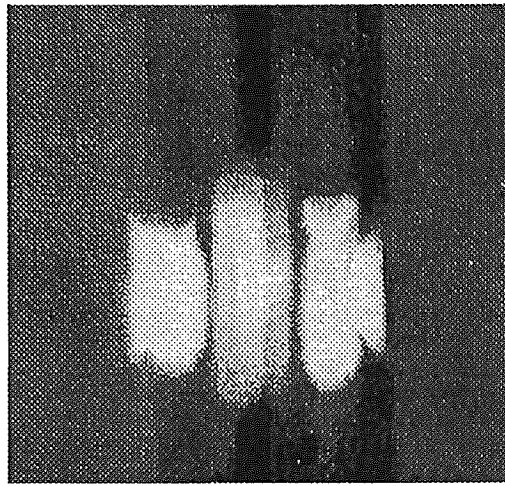
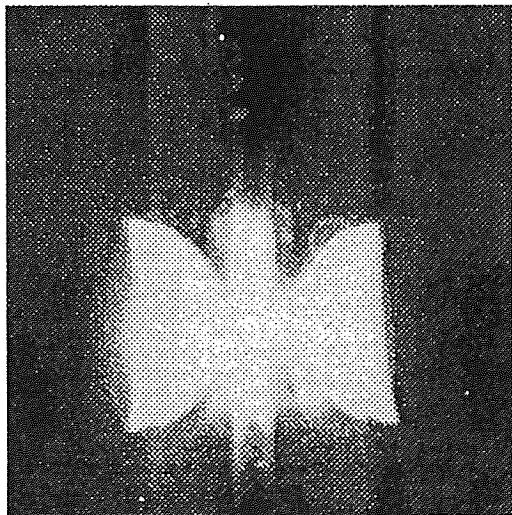
(d) $t = 15.31$ Sec.

(III)

Figure 5 (continued). Effects of the surface roughness on the sealing process (case 4).

gion to reach the melting temperature. This phenomenon leads to a situation where the glass material can no longer move into the cavity. This leads to the bubble formation right next to where the bump is located. Furthermore, a premature temperature drop resulted in the solidification of the glass material on the outer surface of the core region, preventing the upper part of the glass from feeding into the core region. This premature temperature drop is also responsible for the formation of the thermal crack within the seal as seen in Figure 5(e).

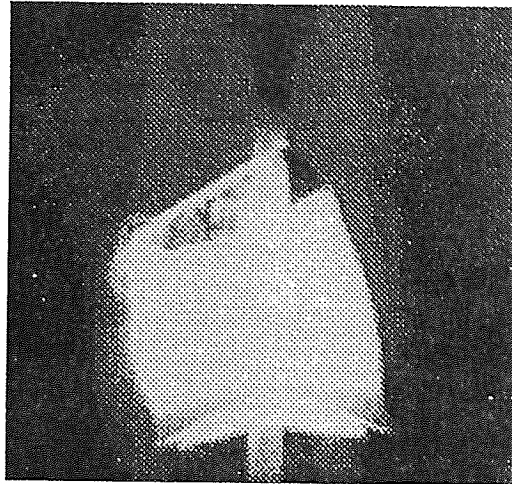
For case 5, the metallic conductor was replaced by a metallic conductor with a smooth surface and there is no bubble formation in the final seal. Referring to Figure 6, which includes detailed images of the sealing process, it can be seen that as the laser beam strikes the outer surface of the glass tube, the temperature of the tube increases. As the temperature reaches the softening point, the inner and outer free surfaces start moving toward the metallic conductor. Meanwhile, the glass material from the upper boundary starts feeding into the core regime due to conduction. In direct contrast to case 4, the glass material moves towards core without any interference. This is because there are no obstacles blocking the feeding flow field. All the void space is filled with glass material entering through the upper boundary. Hence, there is no bubble formation in this case.

(a) $t = 1.56$ Sec.(b) $t = 3.08$ Sec.(c) $t = 4.51$ Sec.(d) $t = 5.20$ Sec.

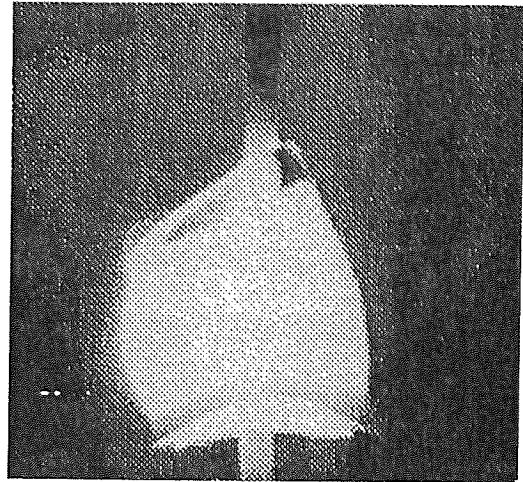
(1)

Figure 6. Effects of the surface roughness (case 5) on removal of bubble formation observed for case 4.

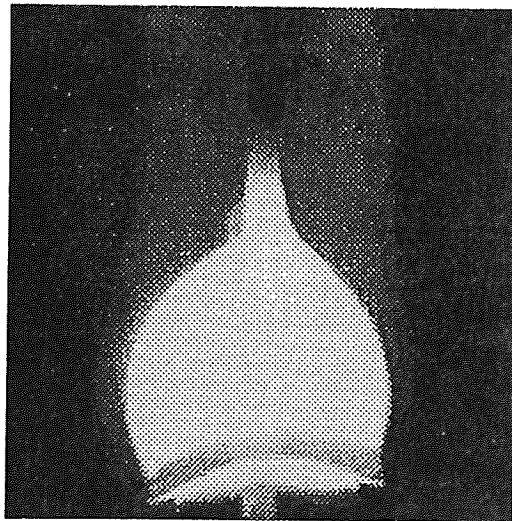
Fig
for



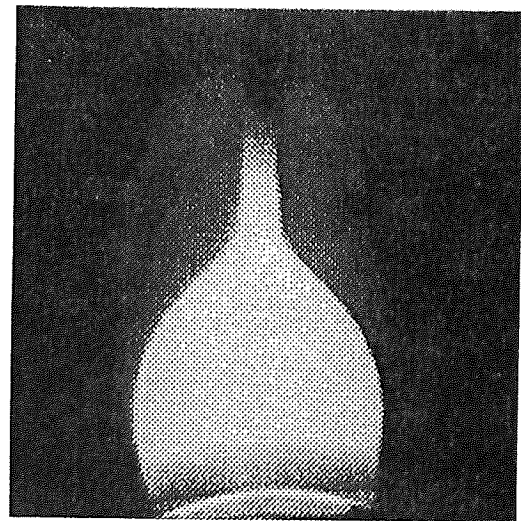
(e) $t = 6.06$ Sec.



(f) $t = 6.37$ Sec.



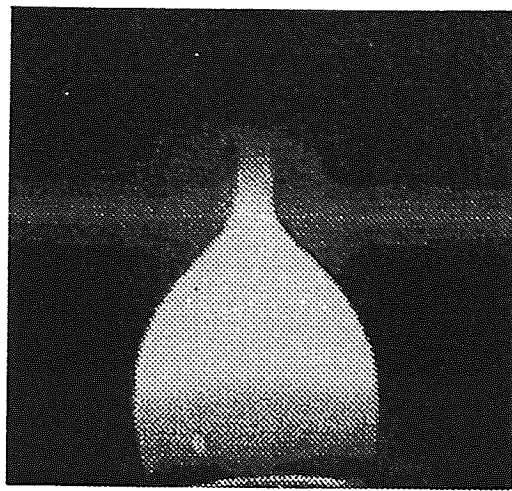
(g) $t = 7.05$ Sec.



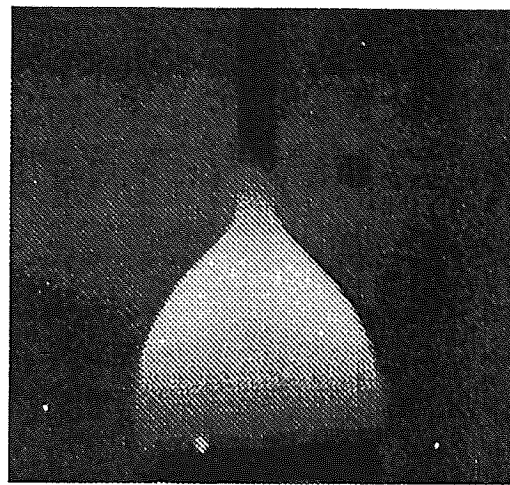
(h) $t = 7.96$ Sec.

(II)

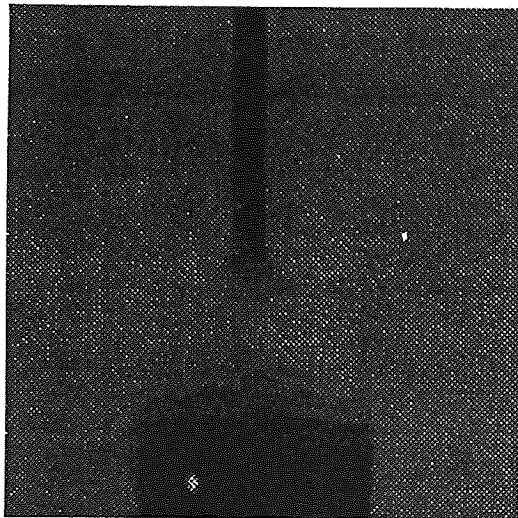
Figure 6 (continued). Effects of the surface roughness (case 5) on removal of bubble formation observed for case 4.



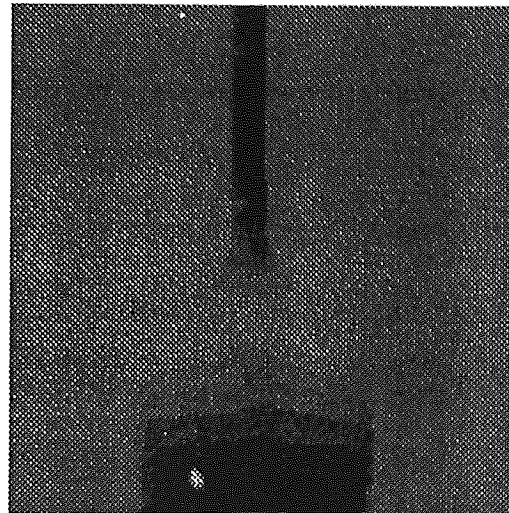
(j) $t = 8.96 \text{ Sec.}$



(i) $t = 10.17 \text{ Sec.}$



(k) $t = 11.35 \text{ Sec}$



(l) $t = 12.43 \text{ Sec.}$

(III)

Figure 6 (continued). Effects of the surface roughness (case 5) on removal of bubble formation observed for case 4.

CONCLUSION

The present work does not follow the conventional research approach in the area of glass-to-metal seals rather it uses a non-conventional point of view to look at the phenomenological information on further understanding of the flow field and free surface movement of the glass with respect to various power supplies and surface roughness of the metallic rod and the occurrence of bubbles in glass-to-metal sealing processes. The outcomes of cases 1 to 5 provide us more information in understanding the mechanisms involved in the sealing process. In this work some pertinent key parameters which had a crucial impact in the final formation of the seals, such as power density of the laser and the surface roughness of the metallic conductors, are isolated and explored in some detail.

By analyzing detailed images of the sealing process, the effect of the power distribution of the heat source and surface roughness of the metallic rod on the quality of the seal were established. The results of the present work will provide ways of identifying and isolating the key regimes in the process, and contributes to a better understanding of the physical mechanisms in-

volved in the sealing process and the related free surface transport and bifurcation phenomena. The results of this work along with the results obtained in the work of Chen and Vafai [7] form a systematic experimental investigation resulting in a better understanding of various parameters involved in the glass-to-metal sealing process.

ACKNOWLEDGEMENTS

The grants from NSF (CTS-8817747) and EWI EES312516 and the educational grant from the U.S. Laser Corporation are acknowledged and greatly appreciated.

REFERENCES

1. Haim, B. Z., G. Grodentzick and Z. Rigbi. 1982. "The Wetting of Metal Surface by a Glass Melt," *Glass Technology*, 23(3).
2. Hrma, P. 1977. "The Kinetics of the Adhesion of Glass to a Solid," *Glass Technology*, 18:4.
3. Wang, M., G. Manzheng, F. Cheng, Z. Yu and Y. Tang. 1986. "The Effect of a Small Amount of Oxide Additives on the Wetting Behavior of Glass on Metal," *Journal of Non Crystalline Solids*, 80:379-386.
4. Bhat, V. K. and C. R. Manning. 1973. "Systems of Na-Fe-SiO₂ Glasses and Steel: 1, Wetting and Adherence," *Journal of the American Ceramic Society*, 56(9):455-458.
5. Hodge, C. E., J. J. Brennan and J. A. Pask. 1973. "Interfacial Reactions and Wetting Behavior of Glass-Iron Systems," *Journal of the American Ceramic Society*, 56(2):51-54.
6. Brennan, J. J. and J. A. Pask. 1973. "Effect of Composition on Glass-Metal Interface Reactions and Adherence," *Journal of the American Ceramic Society*, 56(2):58-62.
7. Chen, S. C. and K. Vafai. 1992. "An Experimental Investigation of Free Surface Transport, Bifurcation and Adhesion Phenomena as Related to a Hollow Glass Ampule and a Metallic Conductor," *Journal of Heat Transfer*, 114(3):743-751.
8. Vafai, K. and S. C. Chen. 1992. "Analysis of Free Surface Transport Within a Hollow Glass Ampule," *Numerical Heat Transfer Part A*, 22(1).
9. Eckert, E. R. G. and Drake. 1972. *Analysis of Heat and Mass Transfer*, New York, NY: McGraw Hill.
10. Kanouff, M. 1987. "Scientific Aspects of Welding," *Sandia Technology*, 11(2):22-27.
11. Buckley, R. G. 1979. "Glass-to-Metal Seals-What You Need to Know," *Ceramic Industry Magazine*, 112:20-23.
12. Miska, K. H. 1976. "How to Obtain Reliable Glass- and Ceramic-to-Metal Seals," *Materials Engineering*, 83:32-35.
13. Vafai, K. 1991. "Analysis of Heat Transfer Phenomena in Glass-to-Metal Seals," *International Communications in Heat and Mass Transfer*, 18:171-184.
14. Product Catalog. 1982. "Schott Technical Glass, Schott Glass Company," West Germany.